Eur. Phys. J. B **27**, 335–340 (2002)
DOI: 10.1140/epjb/e2002-00163-4

THE EUROPEAN PHYSICAL JOURNAL B

Atomic scale characterization of nanostructured a-C:H films

L. Zoppi[1], L. Colombo[1,a], and D. Donadio[2]

[1] Istituto Nazionale per la Fisica della Materia and Department of Physics, University of Cagliari, Cittadella Universitaria, 09042 Monserrato (CA), Italy
[2] Istituto Nazionale per la Fisica della Materia and Department of Materials Science, University of Milano-Bicocca, via Cozzi 53, 20126 Milano, Italy

Received 23 January 2002
Published online 6 June 2002 –

Abstract. Hydrogen incorporation in nanostructured carbon films grown by supersonic cluster beam deposition has been theoretically investigated by classical molecular dynamics. Simulations are shown to enlight the role of the local nanostructure on the formation of hydrogen-related complexes in different carbon environments.

PACS. 61.46.+w Nanoscale materials: clusters, nanoparticles, nanotubes, and nanocrystals – 61.48.+c Fullerenes and fullerene-related materials – 71.15.Pd Molecular dynamics calculations

1 Introduction

Nanostructured carbon films (na-C), grown by supersonic cluster beam deposition (SCBD) [1,2] are extensively investigated because of their peculiar structural [3,4], electronic [5–7], and mechanical [8], properties. Due to their low density porous structure [3,9] the use of such cluster assembled films can be useful in many applications, including micromechanics and microelectronics ones [5,10–12]. More specifically, the presence of nanometric tips embedded in an amorphous graphite-like structure has revealed to be promising for the realization of electron field emission devices [5,6], while the high porosity [13] provides a large specific area for intercalation as needed for electrochemical applications [10]. Patterning of micrometer-size objects [11] and protective coatings for photocathodes [12] represent other two possible applications of such systems.

Na-C films are also useful in the field of energy storage, due to their capability of bonding hydrogen. Recently [14], it has been performed a spectroscopic investigation on na-C samples after reiterated exposures to water vapor and hydrogen: from such studies, it is evident that these films are able to adsorb and to release hydrogen in a reversible way upon moderate heating treatments. It is important to remark that several similar experimental investigations have been addressed to hydrogen physisorption in other carbon based materials [15–17], like nanotubes and nanofibers. Dillon *et al.* [15] first measured the H_2 adsorption capability of an as-prepared soot containing about 0.1 to 0.2 weight% single walls nanotubes (SWNTs), from which an H_2 adsorptivity for pure SWNTs of 5 to 10% has been determined. Chambers *et al.* [17] proposed in turn that tubular, platelet, and herringbone forms of carbon nanofibers are very efficient in adsorption of H_2.

This scenario has stimulated an intense theoretical work mainly aimed at characterizing the local atomic structure in hydrogenated C-based systems, at understanding the H_2 adsorption mechanism, and at evaluating the hydrogen uptake capacity. Bilek *et al.* [18] have studied by first-principles molecular-dynamics (MD) a-C:H samples obtained by quenching from the melt: they found good agreement with neutron-diffraction data as for the position and the magnitude of the H-related features in the pair correlation function. The synthesis of hydrogenated amorphous carbon from molecular precursors has also been investigated by Godwin and Horsfield [19] by means of tight-binding MD: they have characterized various compositions and processing conditions resulting in different hydrocarbon structures. In both cases, the use of quantum mechanical schemes for the description of atomic interactions limits the investigation to a relatively small number of particles, so that it is hard to provide a full description of the relevant features at the nanoscale. As for the evaluation of hydrogen uptake capability, Monte Carlo simulations have been performed on model systems such as carbon nanotubes [20,21] and graphite nanofibers [22,23], focusing on the estimation of hydrogen adsorption capacity. However, none of these simulations confirmed the magnitude of hydrogen adsorption experimentally found by Chambers *et al.* [17] so that the subject is still worthy of investigation. In particular, the actual features of hydrogen inclusions, their dependence upon the local environment and the formation of C_n-H_m complexes is not yet fully understood.

[a] e-mail: luciano.colombo@dsf.unica.it

Table 1. First (1 nn) and second (2 nn) C-C neighbour distances, percentage of three-fold coordinated C-atoms, average coordination (ave. coord.) of C atoms, and C-C-C average bond angle in an a-C:H sample with 20% of H content.

	1nn distance [Å]	2 nn distance [Å]	% of 3-fold coord.	ave. coord.	Bond angle
Ref. [18]	1.460	2.46	73.08	3.05	114.8
This work	1.477	2.56	73.43	2.85	119.5

A major step towards a quantitative atomic-scale characterization of na-C:H structures could derive from the analysis of big computer generated samples, made of a number of atom so large to effectively mimic the real nanoscale structure. This goal can only be reached by moving from quantum to model-potential interaction schemes, as recently proved in describing bulk and surface properties of na-C films [13,24]. Accordingly, in this work we have performed a thorough atomistic simulation study of na-C:H based on the empirical Tersoff potential for C-C, C-H, and H-H interaction [25]. In particular, we have investigated how hydrogen is locally incorporated into a na-C host obtained by direct simulation of the SCBD growth process.

The present investigation has been developed along two directions: (i) the structural characterization of a given na-C sample as function of different hydrogen concentrations; (ii) the investigation – for a given hydrogen concentration – of the structural trends (*e.g.* local atomic coordination, occurrence of C_n - H_m complexes) in different host matrices. This twofold analysis has established a relation between different morphologies of the nanocarbon matrix and the corresponding C-H bonding features.

The paper is organized as follows: in Section 2 we give a brief description of our simulation-strategy and we provide a validation of our model by comparison to previous *ab initio* hydrogenated amorphous carbon (a-C:H) results; in Section 3 we present our results concerning the structural properties of the hydrogenated nanostructured matrices; conclusions are finally drawn in Section 4.

2 Computational details

MD simulations have been carried out by means of an improved version of the Tersoff potential [26] which better models the effects of the local environment on the atom-atom interaction. As for C-H and H-H interactions, we used the parametrization reported in reference [25]. The reliability of Tersoff potential for modelling the structural properties of carbon based materials is well established [13,27]. In order to further validate the present model for hydrogenated systems, we made some preliminary calculations on a-C:H samples obtained by quenching from the melt. More specifically, we chose three a-C:H systems with the same atomic H occurence of of 20% but different mass densities, respectively 1.1 g/cm^3, 2.0 g/cm^3, 3.4 g/cm^3. A simple cubic lattice was chosen as the initial configuration of the atoms, so that a liquid is soon formed by the thermal melting of a such unlikely structure. The system was then aged and equilibrated during a constant MD run at 8000 K for 4 ps. The liquid was finally cooled down to 300 K by using a cooling-rate of 10^{15} K/s (1 δt = 0.2 fs). Similar systems were previously investigated by *ab initio* MD [18], so that a direct comparison is possible.

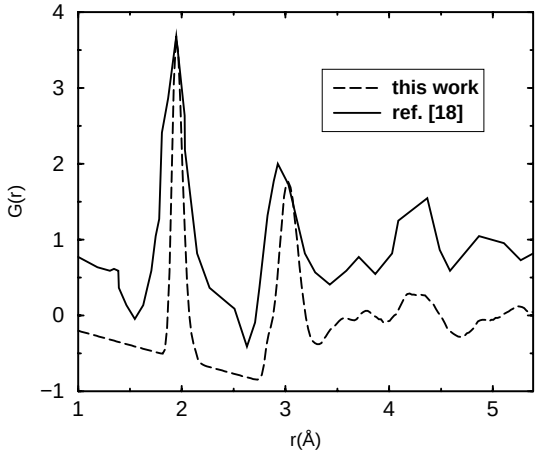

Fig. 1. Comparison between *ab initio* (full line) and present (dashed line) pair correlation function for a quenched-from-the-melt a-C sample with 2.0 g/cm^3 mass density.

In Table 1 we report a direct comparison of atomic properties between *ab initio* and Tersoff data for the sample with 2.0 g/cm^3 density. The present model reproduces quite well the local atomic structure provided by Bilek *et al.* [18] This is further confirmed on a global picture by the pair correlation function reported in Figure 1. We also found, both from average atomic coordination and from bond angle distribution, that going from low density network to high density limit corresponds to a strengthening of the tetrahedral character of the material, due to the increase in the fraction of 4-fold coordinated (sp^3) sites. This is again consistent with *ab initio* data. As for C-H interactions, the value of the nearest-neighbour distance at the density of 2.0 g/cm^3 was 1.09 Å, in very good agreement with 1.1 Å, the *ab initio* value of reference [18]. It is worth noticing that the lower density value (1.1 g/cm^3) which we have considered corresponds nearly to the density value typical of nanostructured carbon films which will be discussed below.

Now let us move to the description of the na-C:H samples which we have investigated in this work. We simulated SCBD growth on a (001) diamond substrate (kept at room temperature) fixing the main features of the molecular beam (*e.g.* cluster vibrational temperature, deposition energy, and cluster mass distribution in the beam) according to the experimental conditions [1]. The simulation cell

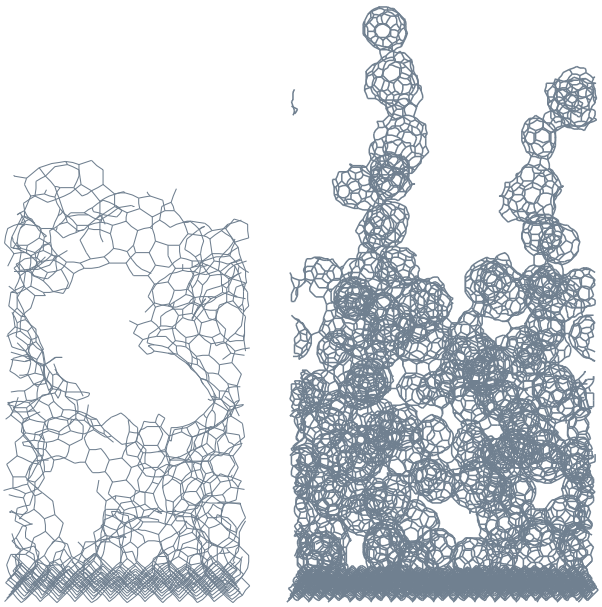

Fig. 2. Atomic structure of amorphous film grown by deposition of beams with unimodal mass distribution and deposition energy of $E_d = 0.1$ eV/atom (sample (a), left) and with bimodal mass distribution with prevalence of big size clusters (sample (c), right).

has been treated as a finite slab along the growth direction (hereafter referred to as z), but as a periodic system along x and y directions. The (001) diamond surface used as substrate has a thickness of 4 atomic layers: the positions of the atoms of the lowest layer are fixed, while the atoms of the second and the third layer are coupled to a thermostat; the top most layer is free of constraints to prevent artifacts in the process of the beam-surface interaction. Further details on the simulation technicalities can be found elsewhere [13].

A first set of films considered in this work has been grown by deposition of cluster beams with unimodal mass distribution (clusters of size corresponding to 1−10 atoms) but different deposition energy, respectively 0.1 eV/atom (sample (a)) and 1.0 eV/atom (sample (b)). We also simulated the deposition of cluster beams with bimodal mass distribution (BMD) (clusters of size corresponding to 1−23 atoms and 46−120 atoms) with relative intensity respectively of 1 : 10 (sample (c)) and 5 : 1 (sample (d)). In both samples (c) and (d) we used a fixed deposition energy of 0.1 eV/atom. In the case of the two films grown by unimodal mass distribution, sample (a) is highly porous showing cavities of nanometric dimension (Fig. 2, left), while sample (b) results to be much more compact; in both cases the fraction of 3-fold sites is ≃70%. As for BMD films, sample (c) shows a porous structure with a random stacking of columnar structures mainly made of covalently bonded fullerenes (Fig. 2, right); while sample (d) shows an amorphous matrix in which it is still possible to recognize fullerenic structures.

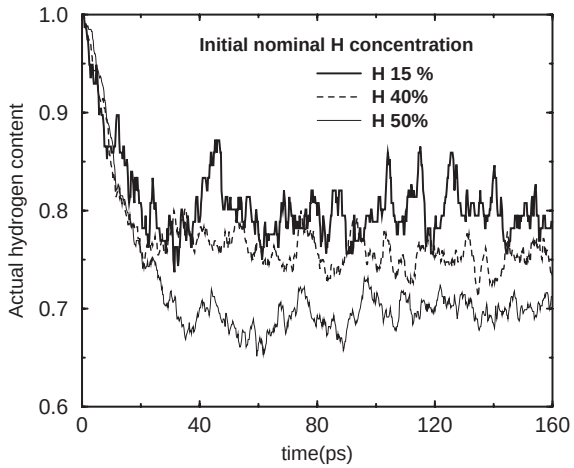

Fig. 3. Variation of the actual hydrogen content (normalized to the initial nominal concentration) in sample (b) upon annealing time.

The hydrogenation procedures consisted in a random insertion of H atoms in the SCBD films, corrected by educated guesses on their initial placements: we avoided to place the next H atom closer to a previous one or to a carbon atom than, respectively, the H-H and C-H nearest neighbor distance as computed in a quenched-from-the-melt sample with similar mass density (1.1 g/cm^3). The nominal hydrogen content has been selected according to experimental data ([19] and references therein). Typically, a-C:H films have a 20−50 at. % hydrogen content: we therefore selected five different H amounts for each SCBD film, ranging from 15% to 50%. After the hydrogen insertion step, na-C:H films have been annealed at finite temperature for 800 000 MD steps (1 time-step = 0.2 fs). We evaluated the actual number of hydrogen atoms within each film every 1000 time-step during the annealing procedure. At the end of the thermalization step, the number of H atoms within each sample reached a saturation value depending on the initial content. In Figure 3 we show the variation of the actual concentration of atomic hydrogen during the annealing process for sample (b). For sake of clarity, we show this trend only for three different initial nominal H concentrations (INHC). As expected, the residual hydrogen percentage (normalized to INHC) at the end of simulation is greater the lower the initial content is. Such an actual post-annealing H concentration (APAHC) is hereafter used to label the various samples investigated and is reported in Table 2.

3 Results

3.1 H distribution along the film growth axis

Each computer generated film was partitioned into layers of 3 Å along the growth direction and a detailed counting of H content for each layer was then carried out. By comparing hydrogen distribution computed as above, we

Table 2. Initial nominal H concentration (INHC) and actual post-annealing H concentration (APAHC) for all computer-generated samples.

Sample	INHC	APAHC
(a)	15	14.0
	25	22.9
	40	30.6
	50	40.3
(b)	15	11.7
	25	17.8
	40	29.5
	50	35.6
(c)	15	12.4
	25	19.1
	40	28.6
	50	33.8
(d)	15	14.6
	25	24.0
	40	36.9
	50	44.7

can observe two different behaviours. In the case of samples with lowest APAHC, we observed a uniform H distribution. Sample (b) only displayed an accumulation of H atoms in the central portion of the film. On the contrary, when samples with high APAHC are considered, we found more intriguing features. Both in sample (c) and (d) a tendency of hydrogen to accumulate at the film-substrate interface region was indeed observed. This effect becomes more sizeable the higher the hydrogen content. In Figure 4 we show this effect for the sample (c): the accumulation in the interface region is clearly visible. A similar trend, quantitavely less important, has also been found in the case of sample (d).

This common feature can be explained by the presence, in both films, of nearly unaffected fullerenes and big size clusters whose packing leaves a lot of empty space in the films. Accordingly, H atoms can easily diffuse through the film and eventually reach the film-substrate interface where a large amount of dangling bonds is offered to hydrogen atoms. Our simulation show that this effect is more evident for sample (c) than for sample (d): this is related to the greater number of big size precursors present in the cluster beam forming sample (c) than sample (d). Although the amount of dangling bonds of the interface region is strongly dependent on the substrate used for the film growth, hydrogen accumulation in the interface region could be very interesting from the experimental point of view. Numerous adhesion tests, performed on cluster assembled films, have found that films with thickness up to 40 μm can be grown on polietylene substrates without delamination [28]. Moreover, recent investigations have shown that thin na-C films may be used as inert strongly bound protective coating for alkali photocathodes [12]. However, our simulations seem to suggest the the hydrogen accumulation in the interface region could cause brittlement which, in turn, possibly cause the detachment of the film from the substrate.

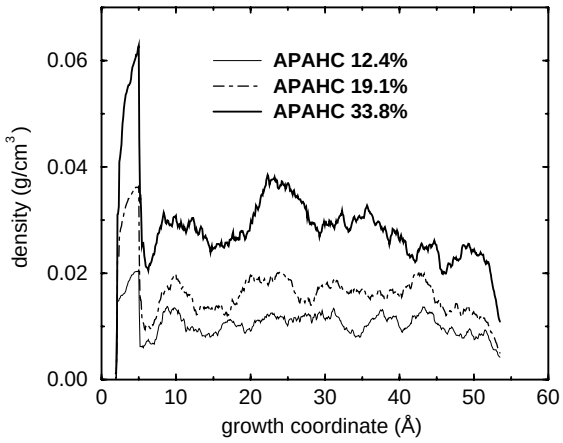

Fig. 4. Hydrogen density along the film growth direction in the case of sample (c) for three different actual post-annealing hydrogen contents (APAHC).

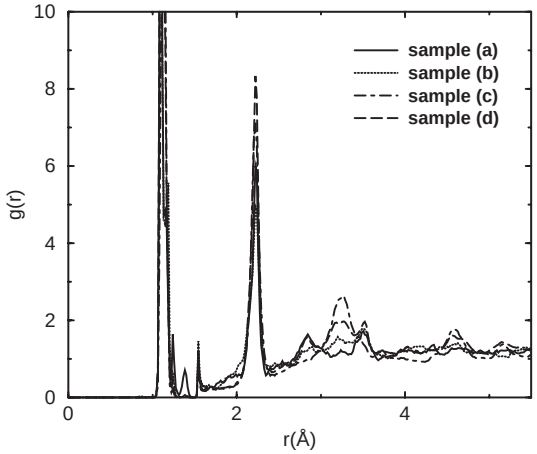

Fig. 5. C-H pair correlation functions evaluated at the lowest APAHC content for each nanostructure.

3.2 Atomic-structure of na-C:H films

In order to investigate local atomic structure, we first determined the equilibrium average lengths of C-H and H-H bonds. To this aim we computed the corresponding pair correlation functions, like that one reported in Figure 5. The bond length values used in the following for determining the local atomic coordinations are 1.4 Å and 0.9 Å for C-H and H-H pairs, respectively. In Figure 6 we show H_2 occurence (%) for each different sample as a function of the APAHC. We found that sample (a) and sample (d) can systematically arrange the largest number of H_2. While sample (a) shows this behaviour also in the lowest APAHC limit, where the percentage of H_2 is about 16% (reaches a value of $\simeq$22% in the limit of high concentration), sample (d) does not seem to promote H_2 formation for low hydrogenation rates. However, as the hydrogen concentration increases, so do the H_2 groups, reaching the value of 17.4% in the highest APAHC limit. As for the behaviour of sample (b) and sample (c), H_2 concentration is almost constant for any configuration, reaching the 10% maximum

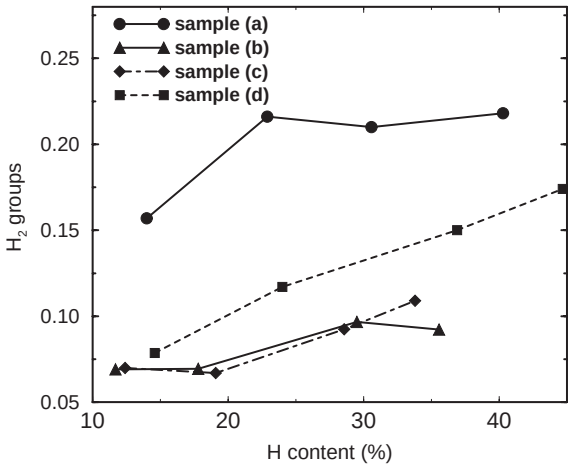

Fig. 6. Relative occurence (%) of H_2 groups found after thermal treatment as function of the actual post-annealing hydrogen content.

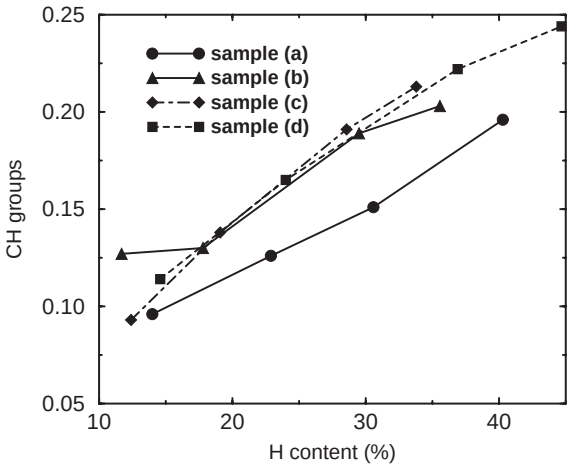

Fig. 7. Relative occurence (%) of C-H groups as function of the actual post-annealing hydrogen content.

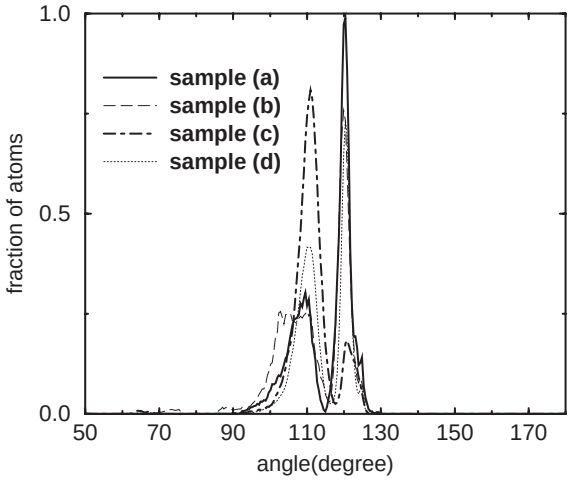

Fig. 8. C-C-H bond angle distribution evaluated at the lowest post-annealing hydrogen content.

value in those sample having the higher total hydrogen concentration.

Although films (a) and (d) have been obtained by means of different growth protocols (unimodal *vs.* bimodal), in both cases most of the precursors are small clusters. Both structures are highly porous, where sample (a) presents cavities of nanometric dimension, while sample (d) shows two kind of cavities: interstitial ones formed by piling up small size clusters and internal ones included within a large cluster. Our calculations proved that H_2 molecules are basically formed in an interstitial cavity, rather than within a cluster cage. This is further confirmed by comparison to sample (c), where mainly cavities of the latter kind are present: as a matter of fact, a quite small amount of H_2 molecules is found in sample (c) despite the large fraction of empty space available within fullerene cages. We attribute this result to the fact that most of the H atoms put into a fullerene cage during the random insertion procedure tend to decorate the inner surface of the cage itself. On the other hand, an external H must overcome an high energy barrier E_b to penetrate within a fullerene cage. We computed E_b for a C_{60} molecule by moving an H atom from the molecule center towards the outside space (through an hexagonal face) finding a value of $E_b \simeq 0.8$ eV. This energy is in fact by far larger than the thermal one available to hydrogen, thus making H accumulation within a cage quite unlikely.

Let us now move to the problem of formation of C_n-H_m groups: our calculations have shown the presence of CH and CH_2. As for CH groups, their percentage increases almost linearly as a function of APAHC for all samples with a tendency to saturation in the highest concentration limit (Fig. 7) where becomes of the order of 20−25%. The same qualitative trend as function of APAHC is also true for CH_2 groups, but their occurence results almost negligible (less than 4%).

Other interesting structural features can been extrapolated from bond angle distribution for C-C-H groups when the pivot atom is a carbon bonded to an H and another carbon atom. In Figure 8 we show the C-C-H bond angle distribution for all the host matrices and lowest APAHC. Two major peaks are observed, one corresponding to 109° (typical of tetrahedral bonding), and the other corresponding to 120° (typical of graphitic structure). In all cases, except for sample (c), there is a clear prevalence of the graphitic coordination respect to the tetrahedral one. Here it is worth reminding that all carbon matrices here investigated consist prevalently of 3-fold sites: accordingly, for sample (a, b), and (d) the formation of C-C-H groups enforces the graphite-like character of the structure; on the contrary, the formation of such complexes seem to promote the diamond-like character of sample (c) film.

4 Conclusions

A fully atomistic structural characterization of hydrogenated nanostructured carbon films has been performed by classical molecular dynamics. We investigated hydrogen features in four different host nanocarbon matrices at

various hydrogen content. The calculations show that the way the hydrogen is locally incorporated strongly depends on the host matrix nanoscale structure. Carbon networks obtained by deposition of fullerenes and other large clusters show an hydrogen accumulation at the film-substrate interface region. We also observed the formation of H_2 and C-C-H groups. We found that H_2 formation is promoted by the presence of interstitial cavities formed by the piling-up of small cluster. Concerning C-C-H groups, the corresponding bond angle distribution indicates that hydrogen could further promote either graphitic (sample (a, b), and (d)) and diamond (sample (c)) coordination. Finally, we report the observation of both CH and CH_2 complexes in all samples with similar and uniform distribution.

We acknowledge many useful discussion with P. Milani. We also acknowledge financial support by MIUR under project PRIN-1999: 'Cluster-assembled carbon nanostructures for advanced applications', and project PRIN-2001 'Nuove frontiere della fisica delle superfici, nanofili e nanocluster'.

References

1. P. Milani, S. Iannotta, *Cluster Beam Syntesis of Nanostructured Materials, Springer Series in Cluster Physics* (Springer-Verlag, Berlin, 1999)
2. P. Milani, M. Ferretti, P. Piseri, C.E. Bottani, A. Ferrari, A. Li Bassi, G. Guizzetti, M. Patrini, J. Appl. Phys. **82**, 5793 (1997)
3. P. Milani, E. Barborini, P. Piseri, C.E. Bottani, A.C. Ferrari, A. Li Bassi, Eur. Phys. J. D **9**, 63 (1999)
4. E. Barborini, P. Piseri, A. Li Bassi, A.C. Ferrari, C.E. Bottani, P. Milani, Chem. Phys. Lett. **300**, 633 (1999)
5. A.C. Ferrari, B.S. Satyanarayana, J. Robertson, W.I. Milne, E. Barborini, P. Piseri, P. Milani, Europhys. Lett. **46**, 245 (1999)
6. A. Ilie, A.C. Ferrari, T. Yagi, S.E. Rodil, J. Robertson, J. Appl. Phys. **90**, 2024 (2001)
7. M. Bruzzi, P. Piseri, E. Barborini, G. Benedek, P. Milani, Diamond Relat. Mater. **10**, 989 (2001)
8. C.E. Bottani, A.C. Ferrari, A. Li Bassi, P. Milani, P. Piseri, Europhys. Lett. **42**, 431 (1998)
9. R. Buzio, E. Gnecco, C. Boragno, U. Valbusa, P. Piseri, E. Barborini, P. Milani, Surf. Sci. **444**, L1 (2000)
10. L. Diederich, E. Barborini, P. Piseri, A. Podestà, P. Milani, A. Schneuwly, R. Gallay, Appl. Phys. Lett. **75**, 2662 (1999)
11. E. Barborini, P. Piseri, A. Podestá, P. Milani, Appl. Phys. Lett. **77**, 1059 (2000)
12. I. Boscolo, P. Milani, M. Parisotto, G. Benedek, F. Tazzioli, J. Appl. Phys. **87**, 4005 (2000)
13. D. Donadio, L. Colombo, P. Milani, G. Benedek, Phys. Rev. Lett. **83**, 776 (1999)
14. C. Lenardi, E. Barborini, V. Briois, L. Lucarelli, P. Piseri, P. Milani, Diamond Relat. Mater. **10**, 1195 (2001)
15. A.C. Dillon, K.M. Jones, T.A. Bekkedahl, C.H. Kiang, D.S. Bethune, M.J. Heben, Nature **386**, 377 (1997)
16. C. Liu, Y.Y. Fan, M. Liu, H.T. Cong, H.M. Cheng, M.S. Dresselhaus, Science **286**, 1127 (1999)
17. A. Chambers, C. Park, R. Terry, K. Baker, N.M. Rodriguez, J. Phys. Chem. B **102**, 4253 (1998)
18. M.M. Bilek, D.R. McKenzie, D.G. McCulloch, C.M. Goringe, Phys. Rev. B **62**, 3071 (2000)
19. P.D. Godwin, A.P. Horsfield, A.M. Stoneham, S.J. Bull, I.J. Ford, A.H. Harker, D.G. Pettifor, A.P. Sutton, Phys. Rev. B **54**, 15785 (1996)
20. F. Darkrim, D. Levesque, J. Chem. Phys. **109**, 4981 (1998)
21. M. Rzepka, P. Lamp, M.A. de la Casa-Lillo, J. Phys. Chem. B **102**, 10894 (1998)
22. Q. Wang, J.K. Johnson, J. Phys. Chem B **103**, 277 (1999)
23. Q. Wang, J.K. Johnson, J. Chem. Phys. **110**, 577 (1999)
24. M. Bogana, D. Donadio, G. Benedek, L. Colombo, Europhys. Lett. **54**, 72 (2001)
25. J. Tersoff, Phys. Rev. B **44**, 12039 (1991)
26. D. Mura, L. Colombo, R. Bertoncini, G. Mula, Phys. Rev. B **58**, 10357 (1998)
27. J. Tersoff, Phys. Rev. Lett. **25**, 2879 (1988)
28. G. Benedek, P. Milani, V.G. Ralchenko, *Nanostructured Carbon for Advanced Applications*, NATO Science Series (Kluwer Academic Press, Dordrecht, 2001)